Environmental and Experimental Botany 200 (2022) 104918

Contents lists available at ScienceDirect

Environmental and Experimental Botany

journal homepage: www.elsevier.com/locate/envexpbot

Low Red to Far-red ratio increases resistance to CO_2 diffusion and reduces photosynthetic efficiency in low light grown tomato plants

Maarten L.J. Wassenaar [a], Wim van Ieperen [a], Steven M. Driever [b,*]

[a] Department of Plant Sciences, Horticulture and Product Physiology Group, Wageningen University, 6700 AA Wageningen, the Netherlands
[b] Department of Plant Sciences, Centre for Crop Systems Analysis, Wageningen University, 6700 AK Wageningen, the Netherlands

ARTICLE INFO

Keywords:
Far-red
Photosynthesis
Tomato
Mesophyll conductance
Red to far-red ratio
Shade, avoidance response
LMA
Photosynthetically active radiation
Photosynthetic, efficiency

ABSTRACT

Application of light-emitting diode technology has opened opportunities to optimize light spectrum for crop production greenhouses and vertical farms. In addition to photosynthetically active radiation, far-red (FR) light has shown potential for enhancing leaf photosynthesis. However, additional FR also alters the red to far-red ratio (R:FR) and induces a shade-avoidance response (SAR) that changes leaf nitrogen, thickness and mass. These acclimations can potentially also alter the resistance to CO_2 diffusion, which can limit photosynthesis. Tomato plants were grown with and without additional FR at two light levels. Changes in photosynthetic responses to light and CO_2 diffusion resistance, as well as leaf mass, thickness and nitrogen content were assessed. At low light additional FR strongly reduced leaf maximum photosynthesis, leaf mass, thickness and nitrogen, and increased the resistance to CO_2 diffusion. These effects were to a much lesser extent present in plants grown at high light intensity. Tomato leaves grown under low light intensity supplemented with FR, show much stronger SAR and a larger increase in CO_2 diffusion resistance than plants grown under high light, which negatively influences their photosynthesis at increasing light intensity. Only if the negative effects of sensitivity to FR and SAR response can be avoided, supplemental FR light may be beneficial to enhance photosynthesis in greenhouse and vertical farm systems.

1. Introduction

The application of energy efficient light-emitting diodes (LED) has become more common in protected cultivation systems over the past decades. It has sparked renewed interest in research on the effects of light quality on crop productivity in controlled environments, as LED lighting allows manipulation of the light spectrum to promote plant photosynthesis and growth.

The part of the spectrum called photosynthetically active radiation (PAR, 400–700 nm) is considered as the main driver of photosynthesis, while far-red light (FR, 700–800 nm) is generally considered non-photosynthetic. Recently, several studies have shown that FR can drive photosynthesis to a certain extent when applied in addition to PAR (Zhen and Bugbee, 2020; Zhen and van Iersel, 2017). This has given rise to the idea that supplementing PAR light with FR light may be useful for increasing photosynthesis and productivity. However, additional FR light also affects the ratio of red (R) to FR (R:FR), which triggers a series of morphological responses, known as the shade avoidance response (SAR) (Trupkin et al., 2014). This response includes stem and petiole elongation, steeper leave angles, reduced branching and early flower induction (Schrager-Lavelle et al., 2016; Trupkin et al., 2014). A shade leaf generally is thinner and has a larger leaf area, with a lower mass per unit area, chlorophyll content, chlorophyll a/b ratios, reduced photosynthetic electron transport capacity, Rubisco content and consequently lower photosynthetic capacity per unit leaf area than sun leaves (Anderson, 1986; Evans and Poorter, 2001; Li et al., 2014; Marchiori et al., 2014). When shaded, the SAR responses naturally allow the plant to compete and maximize the capture of light to increase reproductive success (Devlin et al., 1998; Huber and Wiggerman, 1997; Michaud et al., 2017; Yang et al., 2016). In crop production settings, plants ideally do not compete with each other. So additional FR could be beneficial by driving photosynthesis on the one hand, but could also be counterproductive by triggering SAR and competition on the other hand. In a controlled light environment, light intensity and R:FR can be altered independently. This opens the opportunity to optimize R:FR and light intensity to maximize photosynthetic efficiency.

Apart from light, photosynthesis depends on the capture of CO_2 from the air, which is then converted into carbohydrates by Rubisco and RuBP

* Corresponding author at: Centre for Crop Systems Analysis, Wageningen University & Research, P.O. Box 430, 6700 AK Wageningen, the Netherlands.
E-mail address: Steven.driever@wur.nl (S.M. Driever).

https://doi.org/10.1016/j.envexpbot.2022.104918
Received 14 January 2022; Received in revised form 10 May 2022; Accepted 13 May 2022
Available online 17 May 2022

in the Calvin-Benson-Bassham cycle inside the chloroplast. The ease at which CO_2 diffuses from the air inside the sub-stomatal cavity into the chloroplasts to supply Rubisco is a limiting step in this process and is called mesophyll conductance (g_m). It has been recognized as an important limitation in many species (Flexas et al., 2012, 2008) and any improvement of g_m has been predicted to increase photosynthetic rate, as well as improve water use efficiency (Long et al., 2015; Lundgren and Fleming, 2020).

There are a number of leaf mesophyll components that CO_2 must pass on its diffusion path, such as the cell wall, plasma membrane, cytosol, chloroplast envelopes and chloroplast stroma, each of which presents a resistance to CO_2 diffusion. One of the largest physical determinants of g_m is the surface area of the cells exposed to the intercellular airspace (S_m) and the surface area that is occupied by chloroplasts (S_c) through which CO_2 can diffuse towards the site of Rubisco. S_m is determined to a large extent by the leaf thickness and cell packing, the same factors that largely determine leaf mass per area (LMA). Leaf thickness has been shown to control maximum photosynthetic capacity (Oguchi et al., 2003), which suggests that thicker leaves are favorable for maximal photosynthesis. On the one hand, herbaceous plants with thicker leaves have higher g_m through larger S_m and S_c (Galmes et al., 2013a, 2013b; Terashima et al., 2006). On the other hand, thicker leaves have greater airspace resistance that can eventually limit CO_2 diffusion (Parkhurst, 1994). This indicates that there is a limit to increasing photosynthesis and g_m with regard to leaf thickness for herbaceous species. A meta-analysis of LMA and g_m showed that LMA sets an upper limit on g_m, but also that most herbaceous species have a low LMA and high g_m (Flexas et al., 2008; Galmes et al., 2013b; Parkhurst, 1994; Terashima et al., 2006). In tobacco, a positive relation was observed between LMA and g_m (Evans et al., 1994; Galmes et al., 2013a). However, a negative relation was found in tomato cultivars and wild relatives (Muir et al., 2017, 2014). This discrepancy implies that g_m and LMA may be altered independently to a certain extent in herbaceous species. LMA can be altered by both light intensity and R:FR under LED lighting and could potentially be used to manipulate g_m to increase photosynthetic efficiency. Several studies have grown plants at relatively high light intensity (>500 μmol m^{-2} s^{-1} PAR), while light intensities for shade leaves and as applied by LED lighting in protected cultivation are generally much lower. It therefore raises the question if R:FR can be used under relatively low light intensity to change LMA, as well as leaf thickness, to positively affect g_m and photosynthetic efficiency.

To increase our understanding of how changes in R:FR by supplemental FR light affect LMA, g_m and photosynthetic efficiency, this study investigated the effect of low light intensity and supplemental FR light in tomato, an important herbaceous greenhouse crop. We hypothesize that supplemental FR reduces photosynthetic efficiency, in particular at low light intensity. Tomato plants were grown in controlled conditions under LED lighting with four light treatments, consisting of combinations of two light levels and two R:FR ratios. Photosynthetic efficiency and capacity, g_m, LMA and other leaf traits were measured on youngest fully expanded leaves, to assess treatment effects. Light intensity had a positive effect on leaf thickness, LMA, g_m and photosynthesis and a positive relation was found between both LMA and g_m and g_m and photosynthetic capacity. However, low R:FR had a relatively large negative effect on photosynthetic efficiency of plants grown at low light intensity, accompanied by a low LMA, leaf thickness and g_m. Therefore, supplemental FR reduced LMA, g_m and photosynthetic efficiency at low light intensity in tomato plants.

2. Materials and methods

2.1. Plant material and growth conditions

Seeds of *Solanum lycopersicum* cv Moneymaker were sterilized with alcohol (70%) and bleach (3%), rinsed with tap water and sown in trays with vermiculite wetted with a standard nutrient solution for tomato (electric conductivity (EC) 2.0 Ds/m at 25 °C, pH 5.5). Trays were placed in darkness at 4 °C for 24 h for homogeneous seed imbibition and thereafter placed in a climate chamber for germination at 20 °C, 70% RH, 400 ppm CO_2 and 16 h of photoperiod. Light was supplied by white LEDs (Greenpower LED research module, 15 W white; Philips, the Netherlands) at a light intensity of 150 μmol m^{-2} s^{-1} Photosynthetically Active Radiation (PAR). After 10 days of germination 40 homogeneous seedlings (fully expanded cotyledons stage) were selected and transplanted into four light-separated sub-compartments (2 × 5 plants per sub-compartment) located in the same climate chamber, where they were grown for 4–5 weeks. Sub-compartments varied in light intensity and amount of FR (see Light treatments). Plants were grown on a hydroponic system (collated deep flow system) where the nutrient solution (see above) was circulated for 15 min every half hour and pH and EC were regularly checked. The nutrient solution was replaced upon reaching 10% deviation from setpoint of either pH or EC. Relative humidity, temperature and photoperiod were maintained as described above.

2.2. Light treatments during growth

In total four growth light treatments were given, consisting of treatments with a relatively low light intensity of 75 μmol m^{-2} s^{-1} (LL) and with a relatively high light intensity of 300 μmol m^{-2} s^{-1} PAR (HL), combined with either no FR light (LFR) or additional FR light (HFR). PAR was provided by white LEDs (Greenpower LED research module white, 15 W; Philips, Eindhoven) and additional FR by FR LEDs (Greenpower LED production module far red, 33 W; Philips, Eindhoven). Light emission spectra of both LED-light sources are given in Suppl. Fig. 1. Due to almost complete absence of FR in the white LEDs, calculated R:FR approaches infinity. Therefore instead of R:FR the phytochrome photostationary state (PSS) calculated according to Sager et al. (1988) was used to characterize the FR-level of the light treatments. PSS takes all wavelengths of an incident light spectrum (400–800 nm) into account and their relative involvement in conversions between inactive (P_r) and active (P_{fr}) phytochromes forms and vice versa. As a result PSS also accounts for the phytochrome inactivating effect of blue wavelengths, which are relatively abundant in the emission spectrum of white LEDs. In the growth light treatments with additional FR (HFR) PSS was 0.5–0.6 and without additional FR (LFR) PSS was 0.82. Light intensity and PSS were weekly checked at apex level per light treatment using an spectroradiometer (SS-110, Apogee Instruments, Logan, UT, USA) and adjusted if needed.

2.3. Concurrent measurements of gas exchange and carbon isotope discrimination of CO_2 ($\Delta^{13}C$) to quantify mesophyll conductance

Gas exchange measurements were made by clamping the youngest fully expanded leaf (on the 4th node) of a plant into an open gas exchange system (LI-6400XT, LI-COR, NE, USA), using a 6 cm^2 cuvette with integrated red-blue LED light source (6400–02, LI-COR). Light intensity was set to a photon flux density (PFD) of either 1250 (LL HFR grown plants), 1500 (LL LFR grown plants) or 2000 μmol m^{-2} s^{-1} (all HL grown plants) with 10% blue light. CO_2 concentration of the air entering the leaf chamber was maintained at 400 μmol mol^{-1} and the oxygen concentration at 2% (to minimize the fractionation effect of photorespiration). Flow rate was 350 μmol s^{-1} and leaf temperature maintained at 25 °C. Air vapour pressure inside the leaf chamber was ~2.34 kPa.

Simultaneously, the flow of air for carbon isotope discrimination analysis through the reference line and exhaust air of the leaf cuvette (sample line) was maintained at (200 ml min^{-1}) and CO_2 was purified using two parallel cryogenic CO_2 trapping lines, essentially as described by Kromdijk et al. (2010). Leaves were monitored until net CO_2 assimilation rate (A_n) and stomatal conductance (g_s) had reached a steady state. At steady state, samples of CO_2 were collected and gas exchange parameters were recorded for a period of 15 min. The samples were

collected and sealed in glass tubes using a butane gas torch and stored until analysis, after Borland et al. (1993).

For analysis, the collected sealed glass tubes were broken under vacuum and CO_2 was recollected in sample vials using a cryogenic trapping line. Carbon isotope composition of the collected CO_2 was then analysed using a dual-inlet isotope ratio mass spectrometer (SIRA series II, VG Isotech, modified by Provac Ltd, Crewe, UK).

Observed $\Delta^{13}C$ was calculated from measured gas exchange and isotope composition on the basis of the $^{13}C/^{12}C$ ratios of CO_2 in the reference ($\delta^{13}C_{ref}$) and sample air ($\delta^{13}C_{sam}$), as described by Evans JR et al. (1986):

$$\Delta^{13}C = \frac{1000 \quad \xi \quad (\delta^{13}C_{sam} - \delta^{13}C_{ref})}{1000 + \quad \delta^{13}C_{sam} - \quad \xi \quad (\delta^{13}C_{sam} - \delta^{13}C_{ref})} \tag{1}$$

$$\xi = \frac{C_{ref}}{C_{ref} - C_{sam}} \tag{2}$$

where C_{ref} is the CO_2 concentration of reference air and C_{sam} of the sample air.

Mesophyll conductance (g_m) was calculated as described by Evans and von Caemmerer (2013), with 29‰ for the Rubisco fractionation factor (b) and 12‰ for the photorespiration fractionation factor (f). Mesophyll resistance (r_m) was calculated by taking the inverse of g_m. Measurements were done at 2% O_2 to ensure that the influence of f on the calculation of g_m is small.

2.4. Photosynthetic light response curve

After sampling for $\Delta^{13}C$ determination, rapid photosynthesis light response curves were measured on 2–4 plants per light treatment. PAR supplied by the red-blue LED light source (10% blue) was step-wise reduced to a minimum of ~50 μmol m^{-2} s^{-1} in 10–13 light steps, starting at either 2000 (HL-LFR and HL-HFR), 1500 (LL-LFR) or 1250 (LL-HFR) μmol PAR m^{-2} s^{-1}. At each light intensity step, leaves were monitored until net assimilation rate (A_n) visually reached steady state (usually within 100–200 s) after which a measurement was recorded. The control and settings for gas-composition, leaf temperature and air humidity were similar as described (above) for the concurrent gas exchange measurements during CO_2 sampling for $\Delta^{13}C$ determination.

A non-rectangular hyperbola (Eqs. 1 and 3) (Herrmann et al., 2020; Thornley, 1976), respectively) was fitted on the measured A_n per (absorbed) light intensity and with a constant dark respiration (R_d) to estimate the maximum rate of CO_2 fixation (A_{max}), the maximum quantum yield of CO_2 assimilation at limiting light (ϕ) and a scaling constant for the curvature (θ).

$$\frac{A_n = R_d - \phi \bullet I_{abs} + A_{max} - \sqrt{\left((\phi \bullet I_{abs} + A_{max})^2 - 4 \bullet \phi \bullet I_{abs} \bullet A_{max}\right)}}{2 \bullet \Theta} \tag{3}$$

Fitting was done using the curve_fit() function from the scipy library in Phyton 3.9. The 95% confidence intervals of the estimated parameters were calculated from standard errors obtained from the covariance matrix as supplied by curve_fit, as well as the 95% prediction band of each fitted curve, after clustering and simultaneously fitting all datasets per light treatment. To avoid overfitting and too much influence of the low number of light steps in the linear phase of light response curves in some light treatments, R_d was fixed at 0.5 μmol m^{-2} s^{-1} for all light treatments. Additionally, similar curve fitting was done on all datasets of individual plants to be able to further statistically analyze effects and interaction between light intensity and FR on estimated maximum photosynthesis (A_{max}) by two way Anova.

The quantum yield of CO_2 assimilation (not light-limited), Φ_{CO_2}, was determined according to Genty et al. (1989):

$$\Phi_{CO_2} = \frac{A_n + R_d}{\alpha I} \tag{4}$$

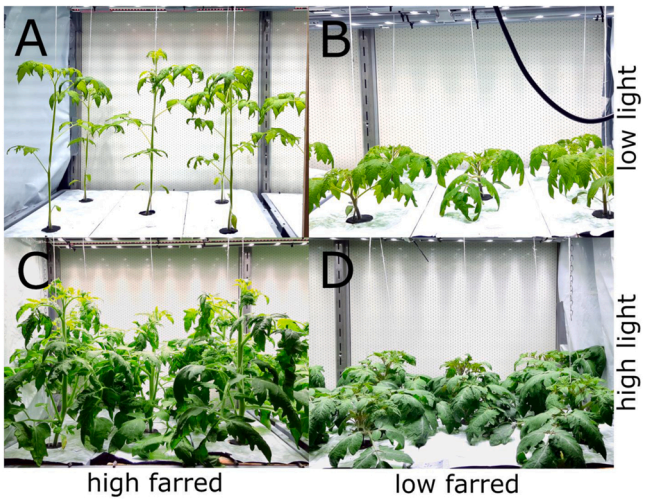

Fig. 1. Photographs of the habit of plants grown at 4 different light intensity × far red combinations, showing clear differences in plant morphology. LL HFR (A), LL LFR (B), HL HFR (C), HL LFR (D) with LL is low intensity (75 μmol PAR m^{-2} s^{-1}), HL high intensity (300 μmol PAR m^{-2} s^{-1}) and LFR is low far red content (PSS 0.82) and HFR high far red content (PSS = 0.55).

where A_n is corrected for respiratory loss (R_d) and divided by the absorbed photon flux (αI), with α as the leaf absorbance.

2.5. Leaf transmission and reflectance

Immediately after measurement of gas exchange, a leaf punch (7.07 cm^2) was taken from measured area of the leaf. This leaf punch was used for measurement of absorptance (α) from 450 to 700 nm, with a dual-channel spectrometer and integrating spheres (Ocean Insights, Rostock, Germany) and a halogen light source (24 V/250 W, type 7748XHP, Philips, the Netherlands). The transmittance (τ) and reflectance (R) for each leaf was used to determine α = (1–R– τ) and total absorbance for the PAR spectrum was calculated, after Webster et al. (2016). Total absorbed light was calculated by combining the percentage of actinic light emitted by the blue (470 nm) and red (640 nm) LEDs in the leaf gas exchange cuvette with α for the respective peak wavelengths, as described by (Naidu and Long, 2004).

2.6. Leaf mass per area, nitrogen content and leaf thickness

After measurement of transmission and reflectance, two leaf punches (14.14 cm^2 total area) were dried at 70 °C for at least 3 days and weighed. From this, the leaf dry mass per area (LMA) was calculated. The dried leaf material was then ground to a fine powder and measured for N content with an elemental analyzer using the Dumas Combustion Method (EA1108 CHN336O, Fisons Instruments).

Leaf thickness was estimated in the growth chamber just before mesophyll conductance measurements with a MultispeQ using protocol RIDES (PhotosynQ inc, East Lancing, MI, USA).

2.7. Statistical analysis

Statistical analyses were performed in R using a two-way analysis of variance followed by a Tukey's HSD post-hoc test to analyse the effects of light intensity and FR on LMA, leaf N content, g_m, g_s and A_{max}. ΦCO_2-light curves were fitted using the loess (fit) function in R, with a 95% confidence interval.

3. Results

Treatments with two light intensities and two far-red levels (FR) had

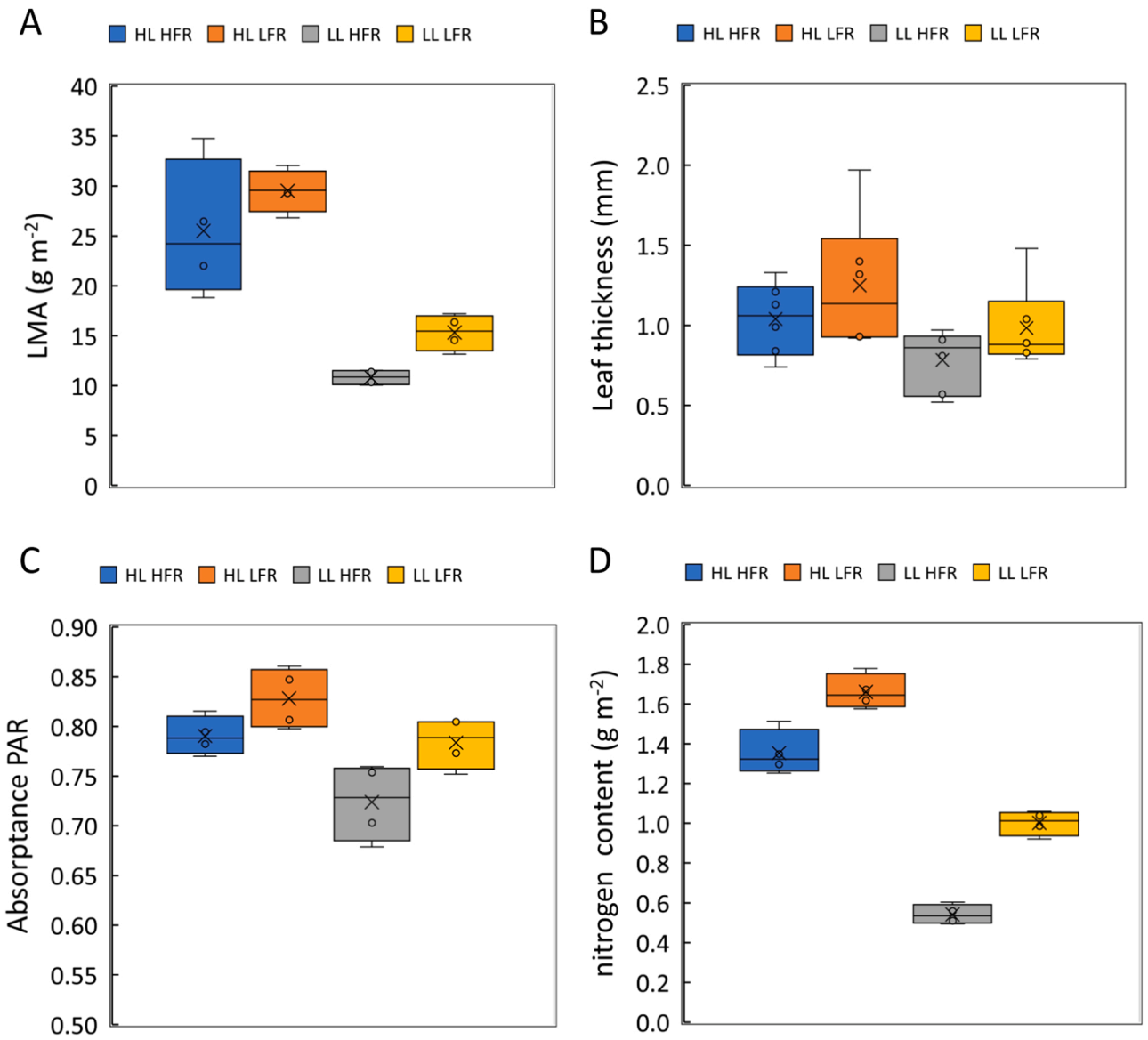

Fig. 2. Boxplot of Leaf Mass per Area (LMA; n = 4, A), mean leaf thickness (n = 6, B), a boxplot of light absorptance (α; n = 4, C) and a boxplot of nitrogen content per treatment (n = 4, D). Colours indicate growth light treatments as explained in Fig. 1: HL HFR (blue), HL LFR (orange), LL HFR (grey), LL LFR (yellow).

clear effects on the growth and morphology. Plants grown at low light intensity (LL) were smaller and thinner (Fig. 1, A and B) than plants grown at high light intensity (HL) (Fig. 1, C and D). Plants at LL had visibly paler and smaller leaves, while plants at HL had visibly darker and larger leaves. The plants grown at high far-red light (HFR) grew taller at both LL and HL (Fig. 1, A and C respectively) than plants grown at low far-red light (LFR) (Fig. 1, B and D). The combination of HFR and LL resulted in plants that were elongated and tall (Fig. 1, A). Plants grown at HFR and HL were elongated similarly, but had thicker stems and leaves (Fig. 1, C). At LFR level and LL, plants did not elongate and had thin stems (Fig. 1, B) and were of similar length to plants grown at HL (and LFR), which had thicker stems (Fig. 1, D). Clear visible differences in growth of the plants were observed in relation to the treatments with LL and HL, combined with LFR and HFR.

The visible differences in growth of plants exposed to combinations of light intensity and FR were also observed at the leaf level. The leaf mass per area (LMA) was statistically significantly different between leaves of plants grown at HL and at LL ($p < 0.001$), irrespective of LFR or HFR (Fig. 2, A). HL grown plants had an LMA ranging from 19 to 35 g m^{-2}, while LL grown plants ranged from 10 to 17 g m^{-2}. However, these differences were less observed in leaf thickness, where average leaf thickness ranged from 0.8 to 1.2 mm (Fig. 2, B).

The absorptance of visible light (450–700 nm, αPAR) was only significantly lower in leaves of plants grown under LL and HFR (Table 1; Fig. 2, C). HL resulted in significantly higher αPAR than LL ($p < 0.001$; 0.79 and 0.83 for HFR and LFR in HL-grown leaves vs.0.71 and 0.78 for HFR and LFR in LL grown leaves). The addition of FR significantly lowered α PAR ($p < 0.002$). Still, there was no interaction effect for light-intensity and FR (Table 1). It is noteworthy that the absorptance for red (640 nm) and blue light (470 nm; αRB) was higher than αPAR for plants from all treatments and that differences between and effects of treatments were similar (Table 1). The spectral absorptance changes observed between treatments were most prominent for the green part of the spectrum (550 nm), where also the largest differences in reflectance and transmittance were found (Suppl. Fig. 2). There was similarity between the pattern of αPAR and LMA between treatments, where also significant effects of light-intensity and FR were found, but no interaction (Table 1). The differences in leaf nitrogen content were largest between HL and LL grown plants (Fig. 2, D), with lower nitrogen content for HFR grown plants. There were significant effects of light and FR, but

Table 1
Summary of a two-way analysis of variance of the effects of light intensity and far red in growth light on leaf mass per area (LMA), leaf thickness, absorptance for PAR and RB (***α***), leaf N content, maximum CO_2 assimilation rate (A_{max}) and mesophyll conductance to CO_2 (g_m).

		LMA		Leaf thickness		α *PAR*		α *RB*		N content		A_{max}		g_m	
Treatment		($g\ m^{-2}$)		(mm)		(-)		(-)		($g\ m^{-2}$)		($\mu mol\ m^{-2}\ s^{-1}$)		($mol\ m^{-2}\ s^{-1}\ bar^{-1}$)	
HL	HFR	25.5	(6.9)	1.04	(0.092)	0.79	(0.02)	0.83	(0.01)	1.35	(0.11)	31.3	(2.44)	0.244	(0.009)
HL	LFR	29.5	(2.2)	1.24	(0.161)	0.83	(0.03)	0.86	(0.02)	1.66	(0.09)	34.8	(0.33)	0.300	(0.036)
LL	HFR	10.8	(0.7)	0.78	(0.079)	0.71	(0.04)	0.76	(0.03)	0.54	(0.05)	12.3	(1.26)	0.109	(0.011)
LL	LFR	15.3	(1.8)	0.98	(0.105)	0.78	(0.03)	0.82	(0.02)	1.00	(0.06)	23.8	(0.86)	0.217	(0.014)
Light		0.000	***	0.036	*	0.001	***	0.000	***	0.000	***	0.000	***	0.000	***
FR		0.043	*	0.094	ns	0.002	**	0.001	**	0.000	***	0.000	***	0.000	***
Light x FR		0.897	ns	0.972	ns	0.195	ns	0.125	ns	0.088	ns	0.002	**	0.026	*

Values are means and standard deviations (in brackets, n = 4). A_{max} are averages of estimates obtained from rapid light-response curves, with R_d fixed at 0.5 $mmol\ m^{-2}\ s^{-1}$. Light intensity on absorbed basis, calculated from incident PAR and absorptance of red blue measuring light for each treatment. Per column, values followed by different letters differ significantly ($p < 0.05$). *** $p < 0.001$; ** $p < 0.01$; * $p < 0.05$.

moderately significant interaction between light and FR ($p = 0.088$, Table 1). The lower nitrogen content of leaves grown at LL confirm the observation of visibly pale green leaves for these plants (Fig. 1, A and B).

The differences in leaf composition in response to the light intensity and FR treatments were accompanied by marked changes in CO_2 assimilation rate (A_n) in response to absorbed light (Fig. 3, A): CO_2 assimilation rate at light saturation (A_{max}) was higher in HL than in LL grown plants (Table 1, and Fig. 3, B and Table 2). The addition of FR during growth strongly reduced A_{max}, but only in LL grown plants: in HL plants the slightly lower A_{max} at HFR was not statically significantly different from A_{max} at LFR (Table 1). A significant interaction effect was found between FR and light intensity ($p = 0.002$). Estimates of ϕ and their 95% confidence intervals for all light treatments are reported in Table 2. Although estimates were higher ϕ for LL LFR grown plants compared to others, the 95% confidence intervals for all treatments were similar. Therefore, no clear differences could be observed between treatments for estimates of ϕ. It is noticeable that 95% confidence intervals were relatively large for all ϕ estimates. Among other causes, it was most likely due to a low number of observations in the (linear) light-limited part of the LRC.

To further investigate the differences in A_n observed above, the mesophyll conductance to CO_2 (g_m) was determined. For HL grown plants, the g_m ranged from 0.23 to 0.34 mol $CO_2\ m^{-2}\ s^{-1}\ bar^{-1}$, while for LL grown plants this ranged from 0.10 to 0.25 mol $CO_2\ m^{-2}\ s^{-1}\ bar^{-1}$ (Fig. 3, C). The g_m of LFR grown plants was relatively higher than of HFR grown plants at the same light intensity. At HL, the difference between HFR and LFR was small (Fig. 3, C; blue and orange, respectively), while at LL this difference was larger (grey and yellow, for HFR and LFR respectively). The observed differences between treatments were statistically significant ($p = 0.026$), which suggests that there was an effect of light intensity, as well as FR level on g_m.

The pattern of g_m in response to light intensity and FR level appears similar to those previously observed for other parameters such as LMA and A_{max}. Indeed, a correlation was observed between g_m and LMA ($R^2 = 0.65$; Fig. 4, A). The lowest observed g_m, as found in LL HFR grown plants, corresponded to the lowest LMA (Fig. 4, A; grey symbols) and the highest g_m to the highest LMA, as found for HL LFR grown plants (Fig. 4, A; orange symbols). A stronger correlation was found for g_m with A_{max} ($R^2 = 0.89$; Fig. 4, B). Here, the lowest and highest g_m values were found to correspond with the lowest and highest A_{max}, which were observed for LL HFR and HL LFR grown plants, respectively (Fig. 4, B; grey and orange symbols, respectively). These correlations suggest an effect of light intensity and FR level treatments on leaf morphology (LMA), A_{max} and g_m. In particular, the correlation between g_m and A_{max} may be indicative of a limitation to CO_2 assimilation imposed by CO_2 diffusion. However, CO_2 diffusion is co-limited by both g_m and stomatal conductance (g_s). To further explore the possible differences in limitation by CO_2 diffusion to A_n as a result of the light intensity and FR levels, the combinations of mesophyll resistance (r_m) and stomatal resistance (r_s) (being the inverse of conductance) were investigated. Resistances were used here because resistances can be summed, in contrast to conductances. The r_s was largest in LL HFR grown plants, which was nearly double the r_s observed for other treatments (Fig. 5, A; orange). Similarly, the r_m of LL HFR grown plants was twice as high compared to other treatments (Fig. 5, A; blue). The sum of r_m and r_s clearly indicated that plants grown at LL and HFR had the highest combined resistance to CO_2, compared to other treatments (Fig. 5, A). However, the relative contribution of r_s and r_m to the total resistance was very similar between treatments, ranging from 55% to 59% for r_m (Fig. 5, B; blue). Despite a doubling of total resistance to CO_2 for LL HFR grown plants, the relative contribution of mesophyll and stomatal resistance remained surprisingly similar.

With regard to A_n and A_{max} a higher total resistance may lead to a lower internal CO_2 concentration at the site of Rubisco in the chloroplast. Therefore, the drawdown of CO_2 concentrations from the air (C_a) to the intercellular airspace (C_i) and the chloroplasts inside the mesophyll (C_c) were compared. There was a slightly larger total drawdown of

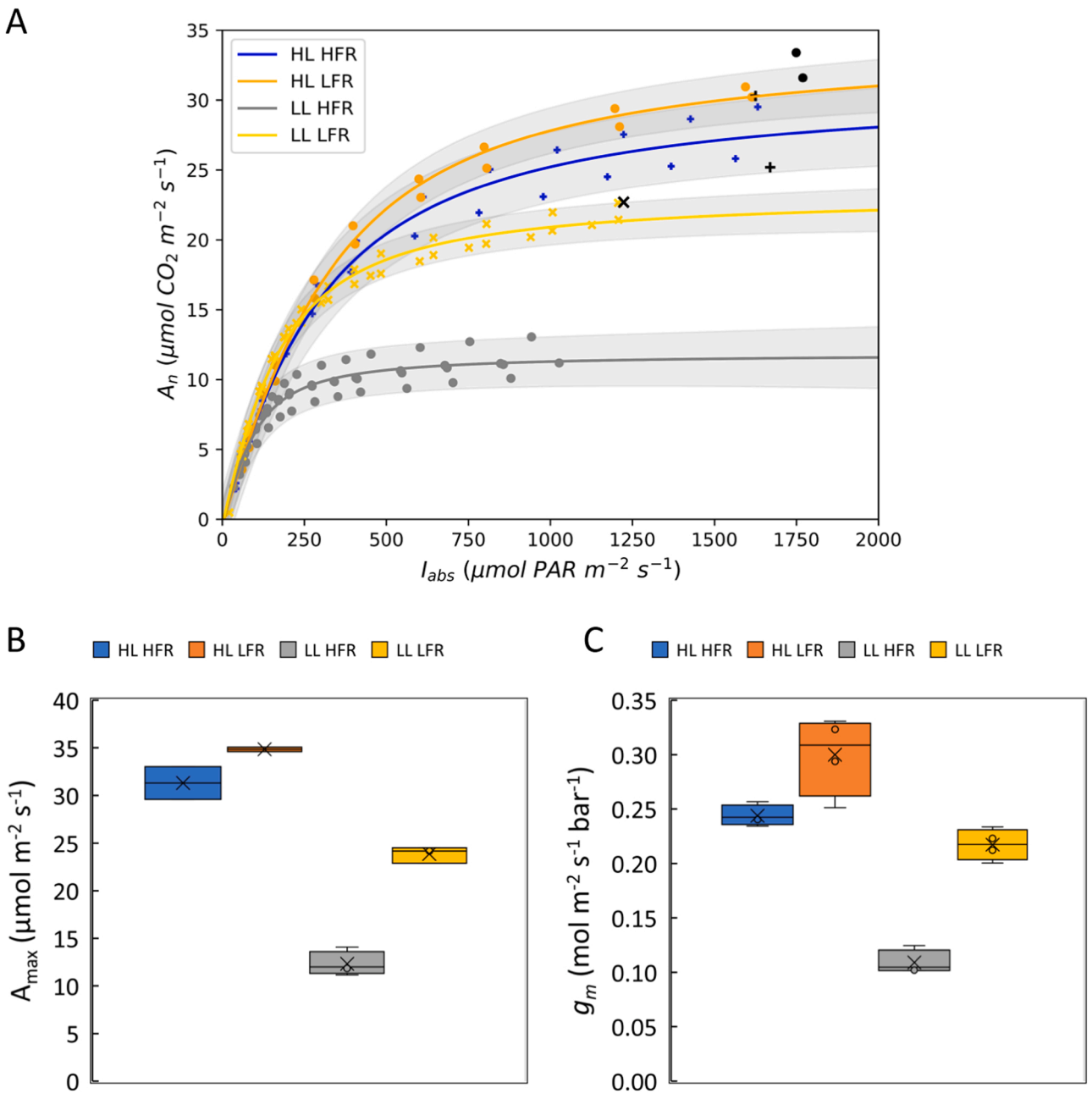

Fig. 3. Light response of net CO_2 assimilation rate (A_n), lines indicate fitted curves with 95% prediction bands per light treatment with measured datapoints in corresponding color. Black symbols are per light treatment measured additional datapoints of A_n at saturating light intensity (during cryo-sampling of CO_2 for $\Delta^{13}C$ of plants when no rapid LRC was measured). For HL HFR: orange curve and • markers. n = 2 for LRC fitting, supplemented with 2 additional datapoints of I_{abs}, A_n measurements at saturating light intensity (black • markers); for HL LFR: blue curve and + marker, n = 2 for LRC-fitting and 2 additional datapoints (2 black + markers); for LL LFR: yellow curves and x-markers, n = 3 for fitting and one additional data point (1 black x marker); and for LL HFR: grey curve and datapoints (•) n = 4 for fitting and no additional datapoints. Boxplots of photosynthetic capacity (A_{max}) (B) and of Mesophyll conductance (g_m) for corresponding light treatments. Statistical analysis for A_{max} and g_m is presented in Table 1, curve fitting and statistical analysis for estimated parameters in Table 2.

CO_2 in plants grown at HL (194 µbar), compared to those grown at LL (181 µbar; Fig. 5, C). The drawdowns between C_i and C_c were very similar (Fig. 5, C; blue), while the drawdowns between C_a and C_i were slightly larger at HL compared to LL grown plants (Fig. 5, C; orange).

The effect on CO_2 diffusion, α and A_n caused by the different growth light intensities and FR levels can be assessed by the overall efficiency by which A_n utilizes light; the quantum yield of CO_2 fixation (ΦCO_2). In response to light intensity, plants had a similar ΦCO_2 for a range of light intensities for all treatments, except for plants grown at LL HFR (Fig. 5, D; grey line and symbols). The combined effect of LL and HFR had a negative effect on the efficiency of CO_2 assimilation.

4. Discussion

Can supplemental FR light during growth be used under relatively low light intensity to change LMA, g_m and photosynthetic efficiency? The tomato plants in this study showed clear differences in response to growth light intensity and FR light, with effects on LMA, g_m and photosynthetic efficiency. Plants grown under HL and LFR had the highest LMA, leaf thickness, α and nitrogen content per leaf area, while the lowest values were found in LL and HFR grown plants. These differences were accompanied by corresponding higher A_{max} and g_m in HL LFR grown plants and lower values in LL HFR grown plants. Across all

Table 2
Effects of Light Intensity and Far Red during growth on the maximum rate of CO_2 fixation (A_{max}), the maximum quantum yield (ϕ) and the scaling constant for the curvature (θ).

Treatment		A_{max} ($\mu mol\ CO_2\ m^{-2}\ s^{-1}$)		ϕ ($\mu mol\ CO_2\ \mu mol\ PAR_{abs}^{-1}$)		Θ (-)	
HL	HFR	31.6	(25.9 – 37.4)	0.086	(0.038–0.134)	0.463	(−0.210 to 1.136)
HL	LFR	34.8	(30.0 – 39.5)	0.083	(0.050–0.116)	0.559	(0.167–0.951)
LL	HFR	12.4	(10.4–14.3)	0.095	(0.045–0.144)	0.656	(0.311 – 1.002)
LL	LFR	23.8	(21.3–26.4)	0.109	(0.070–0.148)	0.537	(0.240 – 0.835)

Parameters are estimates for A_{max}, ϕ and θ after simultaneously fitting all measured datasets of rapid light response curves per light treatment and their 95% confidence intervals. Rapid light response curves were measured at 2% O_2. R_d fixed at 0.5 $\mu mol\ m^{-2}\ s^{-1}$ for fitting. Light intensity on absorbed basis, calculated from incident PAR by the RB light source and the absorptance for red blue measuring light of each treatment (Table 2). Corresponding fitted curves and original data are shown in Fig. 3A.

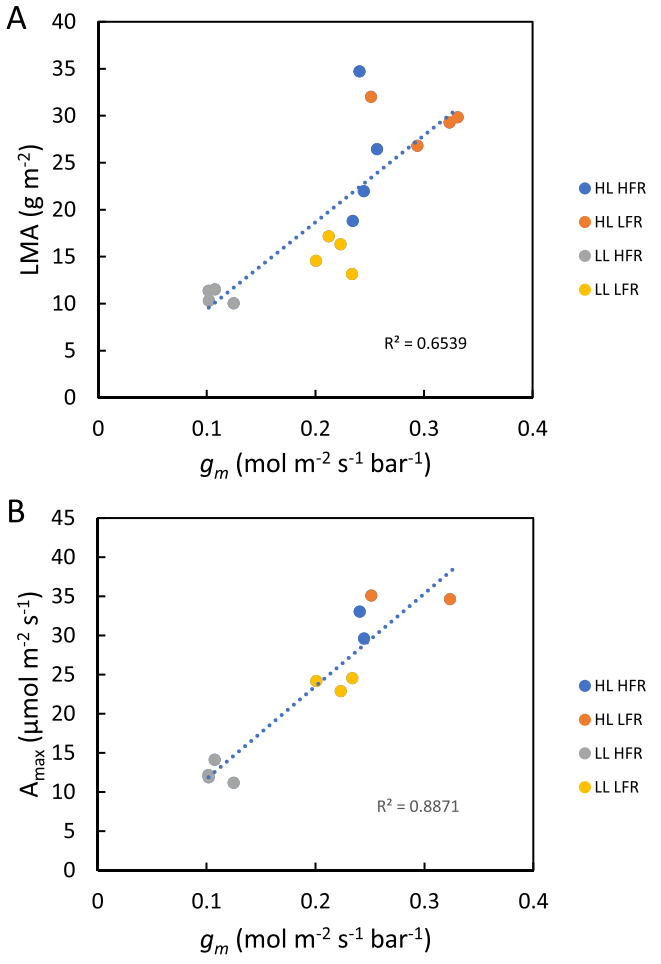

Fig. 4. Correlation graphs between LMA and g_m (A) and between Photosynthetic Capacity (A_{max}) and g_m (B). Colors denote for treatments as described in previous figures. ($p < 0.001$ and $p < 0.001$, for A and B respectively).

treatments, we found positive correlations between LMA and g_m and between A_{max} and g_m. Particularly, LL HFR grown plants had a much lower g_m and significantly lower ΦCO_2 at increasing light intensity compared to plants of other light treatments. Inversely, mean mesophyll and stomatal resistances to CO_2 (r_m and r_s), measured at near-saturating light intensity were larger in LL HFR grown plants compared to the other growth light treatments (Fig. 5, A), but the relative contributions of r_m and r_s to total CO_2 diffusion resistance (Fig. 5, B) and the CO_2 drawdown between ambient air and intercellular spaces (Ca-Ci) and the chloroplast (Ci-Cc) did not differ much from the other treatments (Fig. 5, C). Therefore, supplemental FR during growth decreased LMA, increased CO_2 diffusion resistance and reduced A_{max}, especially at low growth light intensity.

Interestingly, largest relative decrease in ΦCO_2 was found in LL and HFR grown plants, which also showed the strongest SAR (Fig. 1A). A less severe SAR was observed in HL HFR grown plants. This suggests that light intensity can counteract the effects of SAR caused by supplemental FR. SAR increases petiole and leaf length, decreases the leaf mass per leaf area (LMA), and reduces both the leaf chlorophyll content and the chlorophyll *a*:*b* ratio (Evans and Poorter, 2001; Sasidharan et al., 2010; Smith and Whitelam, 1997). In line with this, LL HFR grown plants had the lowest observed values of LMA, as well as leaf nitrogen content and α (indicative of lowered leaf chlorophyll), compared to plants grown with LFR. SAR also caused a large reduction of A_{max} and g_m, which were lowered by more than 50% compared to LFR grown plants (Figs. 3B and 4B, respectively). Previous studies have shown different effects on photosynthesis of additional FR. An increase in photosynthesis was observed in response to supplemental FR in tomato (Kalaitzoglou et al., 2019), soybean (Yang et al., 2018). Others found no effect on photosynthesis in tomato (Ji et al., 2019; Zhang et al., 2019) and lettuce (Jin et al., 2021; Zou et al., 2019). Moreover, both (Ji et al., 2019) and (Kalaitzoglou et al., 2019) concluded that the effect of FR on photosynthesis in the long term was limited. A possible positive effect of FR on photosynthesis as previously proposed (Zhen and Bugbee, 2020; Zhen and van Iersel, 2017) was not seen in the current study, likely also due to the absence of FR in the spectrum of the red blue light used during measurement. Short-term increases in A_n by additional FR reported for lettuce were up to 1.5 $\mu mol\ m^{-2}\ s^{-1}$ (measured at 90 $\mu mol\ m^{-2}\ s^{-1}$ FR and 200 $\mu mol\ m^{-2}\ s^{-1}$ PFD) (Zhen and van Iersel, 2017). Plants can adapt to spectral changes in light by changing the relative size of the two photosystems, to optimize the excitation balance and quantum efficiency of photosynthesis (Hogewoning et al., 2012). However, A_{max} was lowered by HFR by 11.5 $\mu mol\ m^{-2}\ s^{-1}$ in LL grown plants, a reduction of nearly 50%. This decrease is an order of magnitude higher than the short-term enhancement reported for additional FR. Even though no FR was used during measurements, it is unlikely that its absence fully accounts for the reduction in A_{max} at saturating light intensity. It has been reported that chlorophyll, nitrogen content and α in FR-acclimated plants were lowered and that photosynthetic capacity decreased in the long-term (Ji et al., 2019; Zou et al., 2019). In the current study, leaf N content was strongly correlated with A_{max} (Suppl. Fig. 3) and lower leaf nitrogen content was observed in response to supplemental FR. This partly explains the reduction in A_{max} in the presence of FR and LL. However, LMA and g_m were both also reduced and contributed to a reduction in A_{max} especially at LL (Evans et al., 1994; Galmes et al., 2013a).

To further explain the observed effects of FR on A_{max}, conductance to CO_2 by stomata (g_s) and mesophyll (g_m) we assessed by their reciprocal, the resistance (r_s and r_m, respectively) for their contribution to the total CO_2 diffusion resistance. Light treatments resulted in differences in r_m and r_s, which were especially increased at LL with supplemental FR. Remarkably, the relative contribution of r_m and r_s to the total resistance

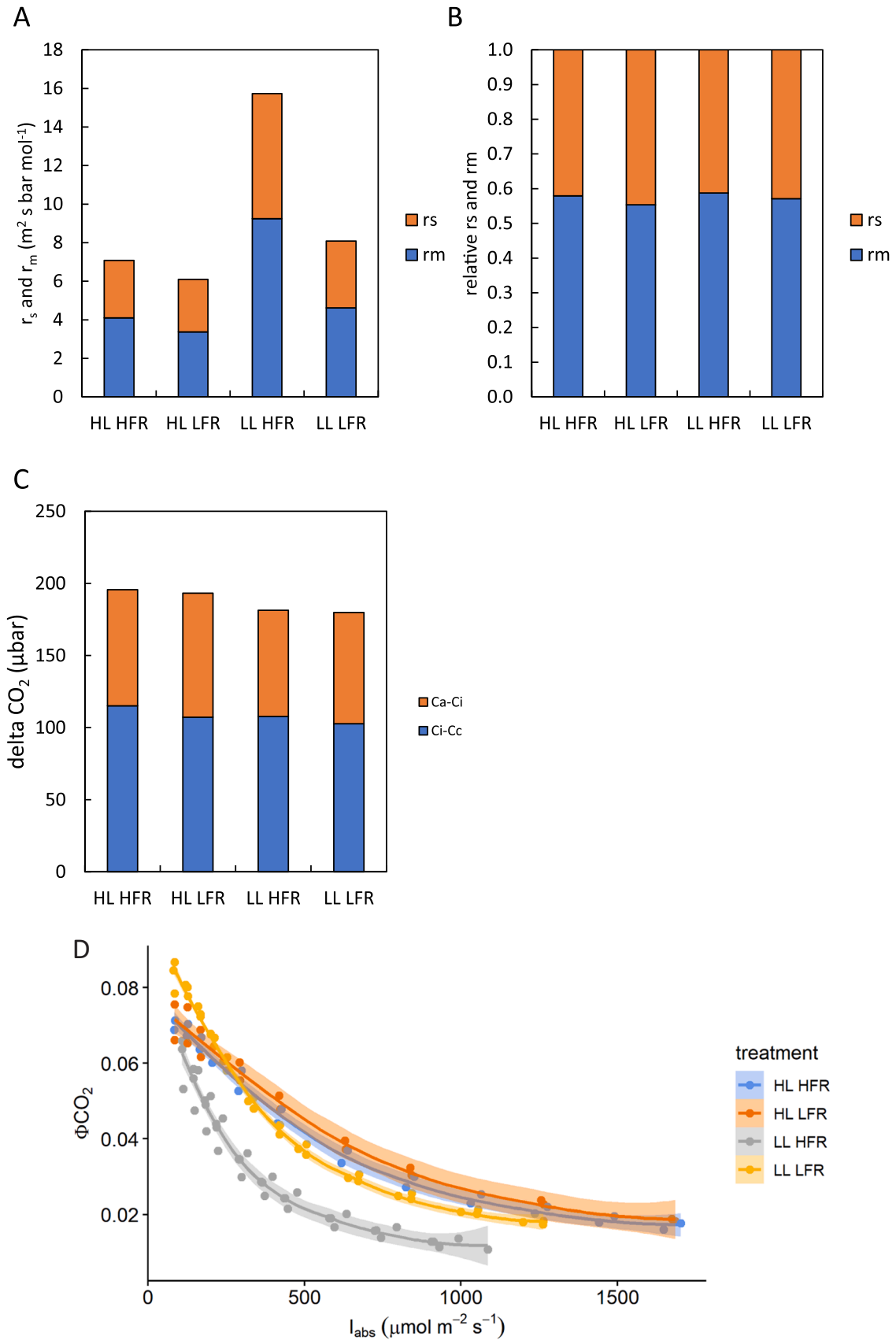

Fig. 5. Mean mesophyll and stomatal resistances to CO_2 (r_m and r_s) per light treatment at high light (A), corresponding relative contributions of r_m and r_s to total resistance for CO_2 diffusion (B) and CO_2 drawdown between CO_2 in the air (C_a), intercellular CO_2 (C_i) and CO_2 within the chloroplast (C_c) (C). Quantum yield of CO_2 fixation (ΦCO_2) in response to absorbed light intensity (D). Colours indicate growth light treatment, lines represent fitted curve with 95% confidence intervals (grey ribbons).

remained constant among the different treatments (Fig. 5B). Moreover, the relative contribution of r_m and r_s, the total resistance and A_{max} resulted in very similar C_i between treatments (Fig. 5C). The similar contributions to total resistance of r_s and r_m has also been found in other studies. A calculation of relative contribution of r_m and r_s of tobacco leaves at different ages from Clarke et al. (2021) showed similar relative contributions of r_s and r_m to total conductance (Suppl. Fig. 4). Indeed, strong correlations between A_n and r_m have previously been found (Barbour et al., 2016; Evans and von Caemmerer, 1996; Evans et al., 1994; Tosens et al., 2012). The widely found correlation indicates a tight co-regulation of A_n and r_m and potentially also r_s. This could explain the constant ratio between A_{max}, r_m and r_s found in both tomato and tobacco. Still, r_s and r_m contributions were determined under steady-state conditions and at high light intensity, which do not reflect the actual behaviour of r_s. Although not directly applicable to controlled environments, this raises the question how r_s changes in relation to r_m under more dynamic and realistic light conditions and how this impacts total resistance.

Across treatments a positive correlation between LMA and g_m was found, which differs from previous studies where no additional FR was used. Negative correlations between LMA and g_m have been found for species with sclerophyllous leaves and high LMA (Hassiotou et al., 2009), and for tomato and tomato-relatives grown in field or greenhouse conditions (Galmes et al., 2011; Muir et al., 2017; Muir et al., 2014). In the current study, the addition of FR caused SAR and altered leaf properties. The differences in LMA-g_m relations may be explained by these properties, as they define how LMA affects g_m in relation to the spatial arrangement of the mesophyll cells (Ren et al., 2019). To a large extent, g_m is determined by leaf anatomy (Evans et al., 2009; Pathare et al., 2020; Terashima et al., 2011) and in particular mesophyll surface area exposed to intercellular airspace (S_m) and chloroplast surface area exposed to intercellular airspace (S_c). Both are dependent on the shape, size and number of mesophyll cells per unit leaf area (Evans, 2021). Similarly, LMA is determined by mesophyll cell number, shape, and mass density, as well as leaf thickness, mesophyll cell layer thickness, cell wall thickness and intercellular airspace (de la Riva et al., 2016; John et al., 2017; Poorter et al., 2009; Veromann-Jurgenson et al., 2017). An increase in LMA caused by more densely packed cells can increase the chance of cell-to-cell contact. This will decrease S_m and inevitably decrease g_m (Flexas et al., 2008; Niinemets et al., 2009; Weraduwage et al., 2016). A positive relation has been observed in tomato plants for g_m and leaf thickness (Galmes et al., 2013a) and leaf thickness has been shown to control maximum photosynthetic capacity (Oguchi et al., 2003). If leaf thickness is large enough to avoid excessive cell–to-cell contact, it is possible to increase S_m and S_c and increase g_m (Peguero-Pina et al., 2017). Although mesophyll cell anatomy is not investigated in the current study, HFR grown plants had thinner leaves than LFR grown plants. This indicates that FR light induces smaller leaf thickness and at LL this was accompanied by the greatest limitation of g_m to A_n. This raises the question whether the reduction in leaf thickness by FR was mediated by reduced S_m and S_c, which would require further detailed study of leaf mesophyll anatomy.

Given the effect of FR on LMA, A_{max} and g_m, can FR light be used as a tool to improve A_{max} in tomato? In previous studies on a range of different species, no significant correlation between LMA and A_n was found (Hassiotou et al., 2010; Nadal et al., 2018; Ren et al., 2019; Veromann-Jurgenson et al., 2017). However, for species with leaves of LMA lower than 100 g m^{-2}, increased LMA was accompanied by increases in S_m and S_c (Ren et al., 2019). In the current study, LMA of tomato leaves varied from 10 to 35 g m^{-2}, which suggests that increased LMA can have a positive effect on g_m. Indeed, a positive correlation was found for LMA with g_m and was accompanied by improved A_{max}. There is also room for enhancement of LMA in tomato. Increases in S_m and S_c together with increased leaf thickness could potentially achieve higher g_m and higher A_{max}. Still, this would require either low levels of FR, or insensitivity to FR to counteract the negative effects of FR observed in this study. As FR is sensed in plants by phytochromes, phytochrome mutants could be used to study the potential for improvement with a lack of FR (sensing) on LMA, mesophyll cell anatomy, g_m and A_{max}.

5. Conclusion

This study found that lowering R:FR during growth by supplemental FR light at low light intensity (LL) caused a SAR and had a negative effect on photosynthesis in tomato plants. Supplemental FR light at LL negatively influences CO_2 diffusion by increasing r_m and r_s, decreasing photosynthesis rates and LMA. If SAR is avoided, supplemental FR may potentially be beneficial for photosynthesis at LL. When the sensitivity for FR can be removed, the lower canopy could be more similar to the LL LFR treatment which was associated with lower r_m and higher A_{max} and could potentially increase photosynthesis. Further studies, e.g. with phytochrome insensitive mutants, are needed to better understand the role that phytochrome sensing plays in this negative effect of FR on LMA, r_m and A_n.

CRediT authorship contribution statement

M.W., W.vI. and S.M.D. conceptualized the study and designed the experiments. M.W. and S.D. validated the isotope discrimination method, carried out the experiments and did the measurements. M.W. and S.D. did the initial data analysis and wrote the manuscript. W.vI. did additional data analysis, reviewed and improved the manuscript. All authors reviewed and approved the manuscript.

Declaration of Competing Interest

The authors declare the following financial interests/personal relationships which may be considered as potential competing interests: Steven M. Driever reports financial support was provided by Wageningen University. Steven M. Driever reports a relationship with Wageningen University that includes: employment, funding grants, and non-financial support. N/A.

Acknowledgements

We like to thank Dr Johannes Kromdijk for helpful discussions and suggestions with setting up the method for carbon isotope discrimination of CO_2 in our lab. We like to thank Dr V. C. Clarke, Dr F.R. Danila and Dr S. von Caemmerer for kind permission for use of their data. This work was financially supported by the Plant Sciences Group Strategic Fund at Wageningen University, the Netherlands.

Appendix A. Supporting information

Supplementary data associated with this article can be found in the online version at doi:10.1016/j.envexpbot.2022.104918.

References

Anderson, J.M., 1986. Photoregulation of the composition, function, and structure of thylakoid membranes. Annu. Rev. Plant Physiol. 37, 93–136.
Barbour, M.M., Evans, J.R., Simonin, K.A., Von Caemmerer, S., 2016. Online CO_2 and H_2O oxygen isotope fractionation allows estimation of mesophyll conductance in C_4 plants, and reveals that mesophyll conductance decreases as leaves age in both C_4 and C_3 plants. N. Phytol. 210, 875–889.
Borland, A.M., Griffiths, H., Broadmeadow, M.S., Fordham, M.C., Maxwell, C., 1993. Short-term changes in carbon-isotope discrimination in the C_3-cam intermediate *Clusia minor* L. Grow. Trinidad Oecologia 95, 444–453.
Clarke, V.C., Danila, F.R., von Caemmerer, S., 2021. Co2 diffusion in tobacco: a link between mesophyll conductance and leaf anatomy. Interface Focus 11, 20200040.
de la Riva, E.G., Olmo, M., Poorter, H., Ubera, J.L., Villar, R., 2016. Leaf mass per area (LMA) and its relationship with leaf structure and anatomy in 34 mediterranean woody species along a water availability gradient. PLoS One 11, e0148788.
Devlin, P.F., Patel, S.R., Whitelam, G.C., 1998. Phytochrome e influences internode elongation and flowering time in arabidopsis. Plant Cell 10, 1479–1487.

Evans, J.R., 2021. Mesophyll conductance: walls, membranes and spatial complexity. N. Phytol. 229, 1864–1876.
Evans, J.R., Kaldenhoff, R., Genty, B., Terashima, I., 2009. Resistances along the CO_2 diffusion pathway inside leaves. J. Exp. Bot. 60, 2235–2248.
Evans, J.R., Poorter, H., 2001. Photosynthetic acclimation of plants to growth irradiance: the relative importance of specific leaf area and nitrogen partitioning in maximizing carbon gain. Plant Cell Environ. 24, 755–767.
Evans JR, S.T., Berry, J.A., Farquhar, G.D., 1986. Carbon isotope discrimination measured concurrently with gas exchange to investigate CO_2 diffusion in leaves of higher plants. Aust. J. Plant Physiol. 13, 281–292.
Evans, J.R., von Caemmerer, S., 1996. Carbon dioxide diffusion inside leaves. Plant Physiol. 110, 339–346.
Evans, J.R., von Caemmerer, S., 2013. Temperature response of carbon isotope discrimination and mesophyll conductance in tobacco. Plant Cell Environ. 36, 745–756.
Evans, J.R., von Caemmerer, S., Setchell, B.A., Hudson, G.S., 1994. The relationship between co_2 transfer conductance and leaf anatomy in transgenic tobacco with a reduced content of rubisco. Funct. Plant Biol. 21, 475–495.
Flexas, J., Barbour, M.M., Brendel, O., Cabrera, H.M., Carriqui, M., Diaz-Espejo, A., Douthe, C., Dreyer, E., Ferrio, J.P., Gago, J., Galle, A., Galmes, J., Kodama, N., Medrano, H., Niinemets, U., Peguero-Pina, J.J., Pou, A., Ribas-Carbo, M., Tomas, M., Tosens, T., Warren, C.R., 2012. Mesophyll diffusion conductance to CO_2: an unappreciated central player in photosynthesis. Plant Sci. 193–194, 70–84.
Flexas, J., Ribas-Carbo, M., Diaz-Espejo, A., Galmes, J., Medrano, H., 2008. Mesophyll conductance to co2: current knowledge and future prospects. Plant Cell Environ. 31, 602–621.
Galmes, J., Conesa, M.A., Ochogavia, J.M., Perdomo, J.A., Francis, D.M., Ribas-Carbo, M., Save, R., Flexas, J., Medrano, H., Cifre, J., 2011. Physiological and morphological adaptations in relation to water use efficiency in mediterranean accessions of solanum lycopersicum. Plant Cell Environ 34, 245–260.
Galmes, J., Ochogavía, J.M., Gago, J., Roldán, E.J., Cifre, J., Conesa, M.À., 2013a. Leaf responses to drought stress in mediterranean accessions of Solanum lycopersicum: anatomical adaptations in relation to gas exchange parameters. Plant, Cell Environ. 36, 920–935.
Galmes, J., Perdomo, J.A., Flexas, J., Whitney, S.M., 2013b. Photosynthetic characterization of rubisco transplantomic lines reveals alterations on photochemistry and mesophyll conductance. Photosynth Res. 115, 153–166.
Genty, B., Briantais, J.-M., Baker, N.R., 1989. The relationship between the quantum yield of photosynthetic electron transport and quenching of chlorophyll fluorescence. Biochim. Et. Biophys. Acta (BBA)-Gen. Subj. 990, 87–92.
Hassiotou, F., Ludwig, M., Renton, M., Veneklaas, E.J., Evans, J.R., 2009. Influence of leaf dry mass per area, CO_2, and irradiance on mesophyll conductance in sclerophylls. J. Exp. Bot. 60, 2303–2314.
Hassiotou, F., Renton, M., Ludwig, M., Evans, J.R., Veneklaas, E.J., 2010. Photosynthesis at an extreme end of the leaf trait spectrum: How does it relate to high leaf dry mass per area and associated structural parameters? J. Exp. Bot. 61, 3015–3028.
Herrmann, H.A., Schwartz, J.-M., Johnson, G.N., 2020. From empirical to theoretical models of light response curves-linking photosynthetic and metabolic acclimation. Photosynth. Res. 145, 5–14.
Hogewoning, S.W., Wientjes, E., Douwstra, P., Trouwborst, G., van Ieperen, W., Croce, R., Harbinson, J., 2012. Photosynthetic quantum yield dynamics: from photosystems to leaves. Plant Cell 24, 1921–1935.
Huber, H., Wiggerman, L., 1997. Shade avoidance in the clonal herb *Trifolium fragiferum*: a field study with experimentally manipulated vegetation height. Plant Ecol. 130, 53–62.
Ji, Y., Ouzounis, T., Courbier, S., Kaiser, E., Nguyen, P.T., Schouten, H.J., Visser, R.G., Pierik, R., Marcelis, L.F., Heuvelink, E., 2019. Far-red radiation increases dry mass partitioning to fruits but reduces *Botrytis cinerea* resistance in tomato. Environ. Exp. Bot. 168, 103889.
Jin, W., Urbina, J.L., Heuvelink, E., Marcelis, L.F., 2021. Adding far-red to red-blue light-emitting diode light promotes yield of lettuce at different planting densities. Front. Plant Sci. 2219.
John, G.P., Scoffoni, C., Buckley, T.N., Villar, R., Poorter, H., Sack, L., 2017. The anatomical and compositional basis of leaf mass per area. Ecol. Lett. 20, 412–425.
Kalaitzoglou, P., van Ieperen, W., Harbinson, J., van der Meer, M., Martinakos, S., Weerheim, K., Nicole, C.C.S., Marcelis, L.F.M., 2019. Effects of continuous or end-of-day far-red light on tomato plant growth, morphology, light absorption, and fruit production. Front. Plant Sci. 10.
Kromdijk, J., Griffiths, H., Schepers, H.E., 2010. Can the progressive increase of C_4 bundle sheath leakiness at low pfd be explained by incomplete suppression of photorespiration? Plant Cell Environ. 33, 1935–1948.
Li, T., Liu, L.N., Jiang, C.D., Liu, Y.J., Shi, L., 2014. Effects of mutual shading on the regulation of photosynthesis in field-grown sorghum. J. Photochem. Photobio. B 137, 31–38.
Long, S.P., Marshall-Colon, A., Zhu, X.G., 2015. Meeting the global food demand of the future by engineering crop photosynthesis and yield potential. Cell 161, 56–66.
Lundgren, M.R., Fleming, A.J., 2020. Cellular perspectives for improving mesophyll conductance. Plant J. 101, 845–857.
Marchiori, P.E.R., Machado, E.C., Ribeiro, R.V., 2014. Photosynthetic limitations imposed by self-shading in field-grown sugarcane varieties. Field Crops Res. 155, 30–37.
Michaud, O., Fiorucci, A.S., Xenarios, I., Fankhauser, C., 2017. Local auxin production underlies a spatially restricted neighbor-detection response in arabidopsis. Proc. Natl. Acad. Sci. U.S.A. 114, 7444–7449.
Muir, C.D., Conesa, M.A., Roldan, E.J., Molins, A., Galmes, J., 2017. Weak coordination between leaf structure and function among closely related tomato species. N. Phytol. 213, 1642–1653.
Muir, C.D., Hangarter, R.P., Moyle, L.C., Davis, P.A., 2014. Morphological and anatomical determinants of mesophyll conductance in wild relatives of tomato (Solanum sect. Lycopersicon, sect. Lycopersicoides; Solanaceae). Plant Cell Environ. 37, 1415–1426.
Nadal, M., Flexas, J., Gulias, J., 2018. Possible link between photosynthesis and leaf modulus of elasticity among vascular plants: a new player in leaf traits relationships? Ecol. Lett. 21, 1372–1379.
Naidu, S.L., Long, S.P., 2004. Potential mechanisms of low-temperature tolerance of c4 photosynthesis in *Miscanthus× giganteus*: an in vivo analysis. Planta 220, 145–155.
Niinemets, U., Wright, I.J., Evans, J.R., 2009. Leaf mesophyll diffusion conductance in 35 australian sclerophylls covering a broad range of foliage structural and physiological variation. J. Exp. Bot. 60, 2433–2449.
Oguchi, R., Hikosaka, K., Hirose, T., 2003. Does the photosynthetic light-acclimation need change in leaf anatomy? Plant Cell Environ. 26, 505–512.
Parkhurst, D.F., 1994. Diffusion of CO_2 and other gases inside leaves. N. Phytol. 126, 449–479.
Pathare, V.S., Koteyeva, N., Cousins, A.B., 2020. Increased adaxial stomatal density is associated with greater mesophyll surface area exposed to intercellular air spaces and mesophyll conductance in diverse c4 grasses. N. Phytol. 225, 169–182.
Peguero-Pina, J.J., Siso, S., Flexas, J., Galmes, J., Garcia-Nogales, A., Niinemets, U., Sancho-Knapik, D., Saz, M.A., Gil-Pelegrin, E., 2017. Cell-level anatomical characteristics explain high mesophyll conductance and photosynthetic capacity in sclerophyllous mediterranean oaks. N. Phytol. 214, 585–596.
Poorter, H., Niinemets, U., Poorter, L., Wright, I.J., Villar, R., 2009. Causes and consequences of variation in leaf mass per area (LMA): a meta-analysis. N. Phytol. 182, 565–588.
Ren, T., Weraduwage, S.M., Sharkey, T.D., 2019. Prospects for enhancing leaf photosynthetic capacity by manipulating mesophyll cell morphology. J. Exp. Bot. 70, 1153–1165.
Sager, J., Smith, W., Edwards, J., Cyr, K., 1988. Photosynthetic efficiency and phytochrome photoequilibria determination using spectral data. Trans. ASAE 31, 1882–1889.
Sasidharan, R., Chinnappa, C., Staal, M., Elzenga, J.T.M., Yokoyama, R., Nishitani, K., Voesenek, L.A., Pierik, R., 2010. Light quality-mediated petiole elongation in arabidopsis during shade avoidance involves cell wall modification by xyloglucan endotransglucosylase/hydrolases. Plant Physiol. 154, 978–990.
Schrager-Lavelle, A., Herrera, L.A., Maloof, J.N., 2016. Tomato phye is required for shade avoidance in the absence of phyb1 and phyb2. Front Plant Sci. 7, 1275.
Smith, H., Whitelam, G., 1997. The shade avoidance syndrome: multiple responses mediated by multiple phytochromes. Plant Cell Environ. 20, 840–844.
Terashima, I., Hanba, Y.T., Tazoe, Y., Vyas, P., Yano, S., 2006. Irradiance and phenotype: comparative eco-development of sun and shade leaves in relation to photosynthetic CO_2 diffusion. J. Exp. Bot. 57, 343–354.
Terashima, I., Hanba, Y.T., Tholen, D., Niinemets, U., 2011. Leaf functional anatomy in relation to photosynthesis. Plant Physiol. 155, 108–116.
Thornley, J.H.M., 1976. Mathematical Models in Plant Physiology: A Quantitative Approach to Problems in Plant and Crop Physiology. Academic Press.
Tosens, T., Niinemets, U., Vislap, V., Eichelmann, H., Castro Diez, P., 2012. Developmental changes in mesophyll diffusion conductance and photosynthetic capacity under different light and water availabilities in *Populus tremula*: how structure constrains function. Plant Cell Environ. 35, 839–856.
Trupkin, S.A., Legris, M., Buchovsky, A.S., Tolava Rivero, M.B., Casal, J.J., 2014. Phytochrome b nuclear bodies respond to the low red to far-red ratio and to the reduced irradiance of canopy shade in arabidopsis. Plant Physiol. 165, 1698–1708.
Veromann-Jurgenson, L.L., Tosens, T., Laanisto, L., Niinemets, U., 2017. Extremely thick cell walls and low mesophyll conductance: welcome to the world of ancient living! J. Exp. Bot. 68, 1639–1653.
Webster, R.J., Driever, S.M., Kromdijk, J., McGrath, J., Leakey, A.D., Siebke, K., Demetriades-Shah, T., Bonnage, S., Peloe, T., Lawson, T., 2016. High C_3 photosynthetic capacity and high intrinsic water use efficiency underlies the high productivity of the bioenergy grass *Arundo donax*. Sci. Rep. 6, 1–10.
Weraduwage, S.M., Micallef, M.C., Marillia, E.F., Taylor, D.C., Grodzinski, B., Micallef, B. J., 2016. Increased mtpdh activity through antisense inhibition of mitochondrial pyruvate dehydrogenase kinase enhances inflorescence initiation, and inflorescence growth and harvest index at elevated CO_2 in *Arabidopsis thaliana*. Front Plant Sci. 7, 95.
Yang, D., Seaton, D.D., Krahmer, J., Halliday, K.J., 2016. Photoreceptor effects on plant biomass, resource allocation, and metabolic state. Proc. Natl. Acad. Sci. U.S.A. 113, 7667–7672.
Yang, F., Feng, L., Liu, Q., Wu, X., Fan, Y., Raza, M.A., Cheng, Y., Chen, J., Wang, X., Yong, T., 2018. Effect of interactions between light intensity and red-to-far-red ratio on the photosynthesis of soybean leaves under shade condition. Environ. Exp. Bot. 150, 79–87.
Zhang, Y.-t, Zhang, Y.-q, Yang, Q.-c, Tao, L., 2019. Overhead supplemental far-red light stimulates tomato growth under intra-canopy lighting with leds. J. Integr. Agric. 18, 62–69.
Zhen, S., Bugbee, B., 2020. Substituting far-red for traditionally defined photosynthetic photons results in equal canopy quantum yield for CO_2 fixation and increased

photon capture during long-term studies: implications for re-defining par. Front Plant Sci. 11, 581156.
Zhen, S., van Iersel, M.W., 2017. Far-red light is needed for efficient photochemistry and photosynthesis. J. Plant Physiol. 209, 115–122.
Zou, J., Zhang, Y., Zhang, Y., Bian, Z., Fanourakis, D., Yang, Q., Li, T., 2019. Morphological and physiological properties of indoor cultivated lettuce in response to additional far-red light. Sci. Hortic. 257, 108725.